ChemComm

IYC 2011
International Year of CHEMISTRY

This article is part of the

# Supramolecular Chemistry web-based thematic issue

celebrating the International Year of Chemistry 2011

Guest editors: Professors Philip Gale, Jonathan Sessler and Jonathan Steed

All articles in this issue will be gathered together online at www.rsc.org/chemcomm/supra.

ChemComm

Dynamic Article Links

Cite this: *Chem. Commun.*, 2011, **47**, 5988–5990

www.rsc.org/chemcomm

COMMUNICATION



# Manganese(II) complexes of scorpiand-like azamacrocycles as MnSOD mimics†

**Mª Paz Clares,[a] Salvador Blasco,[a] Mario Inclán,[a] Lucas del Castillo Agudo,[b] Begoña Verdejo,[a] Conxa Soriano,[b] Antonio Doménech,[a] Julio Latorre[a] and Enrique García-España*[a]**

***Received 26th January 2011, Accepted 11th April 2011***
**DOI: 10.1039/c1cc10526d**

**$Mn^{II}$ complexes of scorpiand-type azamacrocycles constituted by a tretrazapyridinophane core appended with an ethylamino tail including 2- or 4-quinoline functionalities show very appealing *in vitro* SOD activity. The observed behaviour is related to structural and electrochemical parameters.**

Aerobic living systems need molecular dioxygen to generate all the energy required for their metabolic processes. Higher organisms have such a high $O_2$ consumption that they need a continuous supply of this element for their survival. Paradoxically, the existence of an oxygenated atmosphere represents a danger to life. Dioxygen has enough oxidant capacity to oxidize organic substances in an exoergonic way. If this does not occur, it is due to the kinetic inertness produced by the mismatch between the paramagnetic dioxygen molecule and diamagnetic living matter. Nevertheless, four-electron reduction of dioxygen to water leads to the formation of diamagnetic peroxo intermediate species that are toxic to living organisms (ROS species). The formation of these toxic species is related to the aging of living organisms and diseases like amyotrophic lateral sclerosis (ALS), which leads to the progressive degeneration of motor neurons.[1] There is extensive evidence that oxidative stress is also a key event in the pathogenesis and exacerbation of Alzheimer's Disease (AD).[2] In order to scavenge or find useful roles for these species living organisms have developed a battery of protective enzymes, such as superoxide dismutases (SODs), catalases and peroxidases.

SOD enzymes accelerate superoxide dismutation into hydrogen peroxide and molecular dioxygen. Three different isoforms of SOD have been found in mammals. While SOD1 (or Cu/Zn SOD) and SOD3 (or EC-SOD) have copper and zinc in their catalytic centre, SOD2 (MnSOD) has manganese in its active site and is exclusively associated with mitochondria. The importance of SOD2 is highlighted by the fact that in contrast to SOD1 and SOD3, SOD2 knockout is lethal to mice.[3]

Although application of SOD enzymes to animals has beneficial effects for some of the above-mentioned diseases, until now this treatment has been shown not to be applicable for humans due to severe complications mainly related to allergic responses. Low molecular weight mimics could have significant advantages with respect to SOD enzymes such as lack of immunogenic responses, longer half-life in the blood, improved access to cells and intercellular space, low cost, *etc.*[4] Some of the most relevant low molecular SOD mimics are complexes of polyamine ligands of either cyclic or open-chain topology.[5] A particularly relevant example is the complex M40403 included in Chart 1.[6] In this respect, we have found that some of our polyamine compounds might display an interesting behaviour as SOD mimics.[7] Here we present a series of novel aza-macrocycles of the so-called scorpiand class[8] that show significant potentiality as MnSOD mimics (Chart 1).

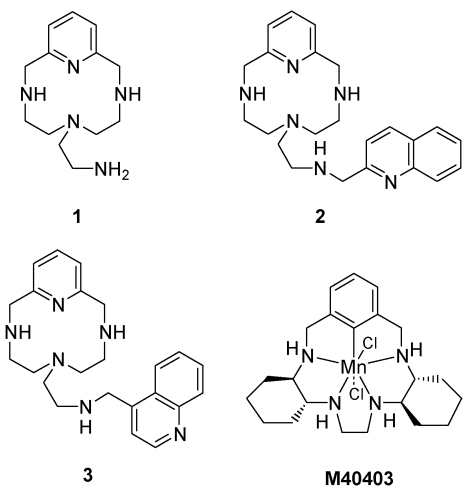


**Chart 1**

[a] *Instituto de Ciencia Molecular, Departamento de Química Inorgánica, Universidad de Valencia, C/Catedrático José Beltrán 2, 46980, Paterna (Valencia), Spain. E-mail: enrique.garcia-es@uv.es*
[b] *Departamentos de Química Orgánica y Microbiología y Ecología, Facultad de Farmacia, Universidad de Valencia, Avda. Vicente Andrés Estellés s/n, 46100, Burjassot (Valencia), Spain*

† Electronic supplementary information (ESI) available: Description of the synthesis and characterization of compounds **2** and **3**. Protonation constants and NMR variation of compounds **2** and **3**. Synthesis of the structures (**4**) and (**5**). Details of X-ray data collection. CCDC 810034 and 810035. For crystallographic data in CIF or other electronic format see DOI: 10.1039/c1cc10526d

Compounds **2** and **3**[9] were synthesised by reaction of precursor compound **1**[10] with the corresponding monoaldehydes followed by reduction with $NaBH_4$. Synthetic details, characterization data and protonation constants determined by pH-metry for the new macrocycles **2** and **3** have been deposited in the ESI.†

Compounds **1–3** interact in water with $Mn^{II}$ yielding stable complexes that undergo atmospheric oxidation very slowly, particularly in the cases of **2** and **3**. pH-Metric studies carried out in 0.15 M $NaClO_4$ at 298.1 K have allowed us to infer the speciation model and values of the stability constants[11] gathered in Table S2 (see ESI†).

The distribution diagrams collected in the ESI† (Fig. S2) show that for a 1 : 1 molar ratio the complexes are quantitatively formed above pH 7.

Slow evaporation of aqueous solution containing $MnSO_4$, $NaClO_4$ and either **2** or **3** at a pH value of *ca.* 8 led to the formation of crystals of $[Mn(\mathbf{2})](ClO_4)_2$ (**4**) or $[Mn(\mathbf{3})(H_2O)](ClO_4)_2$ (**5**) suitable for X-ray analysis (see ESI†). The crystal structure of **4** consists of $[Mn(\mathbf{2})]^{2+}$ complex cations and perchlorate counter-anions. $Mn^{II}$ is coordinated to the four nitrogen atoms of the macrocycle, to the secondary amino group of the bridge and to the nitrogen atom of the quinoline moiety with a rather non-symmetrical coordination geometry. The Mn–N bond distances rank from 2.15 to 2.33 (see Fig. 1 and Table S4A, ESI†, for selected bond distances and angles).

The crystal structure of **5** presents remarkable differences with respect to **4**. First, as it could be anticipated, the quinoline nitrogen is not implicated in the coordination to $Mn^{II}$, which completes its hexacoordination with a water molecule (Fig. 2). Moreover, in **5** the coordination geometry around the metal ion, although distorted is closer to a regular octahedral geometry than in **4**. The angles between adjacent atoms in the coordination sphere rank from 72.5° to 109.2°. The shortest distance in the coordination sphere is Mn–O1 (2.08 Å) and the longest ones are those with the secondary amino groups of the macrocycle (Table S5A, ESI†). The water molecule is further stabilized in the solid state by hydrogen bonding with a quinoline N6 nitrogen coming from a neighbor molecule and with an oxygen of a perchlorate counter-anion. Unlike **4**, the coordination site of **5** is fully accessible by substrates that can either increase the coordination number of $Mn^{II}$ or replace the coordinated water molecule.

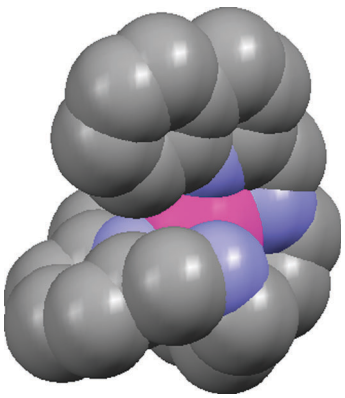

**Fig. 1** Spacefill representation of the structure of the $[Mn(\mathbf{2})]^{2+}$ cation.

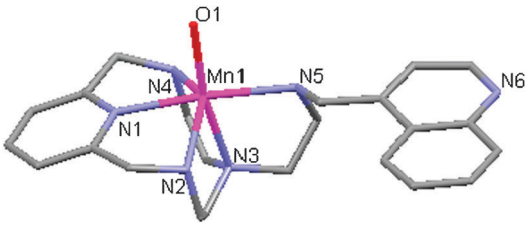


**Fig. 2** Stick representation of the structure of the $[Mn(\mathbf{3})(H_2O)]^{2+}$ cation.

The presence of a water molecule in the coordination sphere of $Mn^{II}$ is reminiscent of the MnSOD enzyme site[12] which, as it will be shown later, plays a significant role in SOD activity.

The cyclic voltammetric response of the Mn–**1**, Mn–**2** and Mn–**3** systems at biological pH values consists of an anodic peak at *ca.* +0.50 V coupled with a weak cathodic counterpart at +0.44 V, often followed by additional weaker cathodic signals. The main couple at *ca.* +0.50 V can be described in terms of an essentially reversible one-electron oxidation as judged by the anodic-to-cathodic peak potential separation (60 mV) and the independence of the midpeak potential with the potential scan rate ($5 < v < 500$ mV $s^{-1}$). The peak potentials ($E_p$) become negatively shifted on increasing the pH, so that linear $E_p$ *vs.* pH are obtained ($6 <$ pH $< 10$). The slope of such representations (60 mV $decade^{-1}$) denotes that a one-proton, one-electron reversible oxidation process occurs. The appearance of weaker cathodic peaks suggests that the electrochemical oxidation of the parent $Mn^{II}$ complex process leads to the formation of a $Mn^{III}$ analogue which undergoes a relatively slow dissociation and/or structural rearrangement (EC mechanism).

Although the formal electrode potentials for the $Mn^{III}/Mn^{II}$ couples fall within the optimal range for SOD activity (Table 1), they depart from the midway potential (+360 mV *vs.* SHE) for the oxidation and reduction of $O_2^-$, being closer to the upper limit of +0.86 V.[13] Electrode potentials close to the midway one would be the most adequate from thermodynamic grounds.[14] However, it has been stated that higher potentials are required for achieving a more selective $O_2^-$ removal. Such higher potentials would prevent oxidation of the resting $Mn^{II}$ oxidation state by other biologically relevant oxidizing species such as nitric oxide, peroxynitrite, hydrogen peroxide, hypochlorite or oxygen.[15]

Solid state electrochemistry of **5** was performed following the voltammetry of microparticles approach[16] upon formation

**Table 1** $IC_{50}$, $k_{cat}$ and $E$ $Mn^{III}/Mn^{II}$ values obtained for the systems Mn–**1**, Mn–**2**, Mn–**3** and M40403

| Reaction | $IC_{50}$/μmol $L^{-1}$ | $k_{cat}$/$mol^{-1}$ $L^1$ $s^{-1}$ | E (V *vs.* SHE) |
|---|---|---|---|
| Mn–**1** | 2.21 | $1.5 \times 10^{6}$[b] | +0.66 |
| Mn–**2** | 1.17 | $3.0 \times 10^{6}$ | +0.85 |
| Mn–**3** | 0.30 | $1.5 \times 10^{7}$ | +0.68 |
| M40403[a] | | $2.0 \times 10^{7}$ | +0.74 |

[a] Values taken from ref. 4. [b] Errors in the $k_{cat}$ values are estimated to be ±5%.

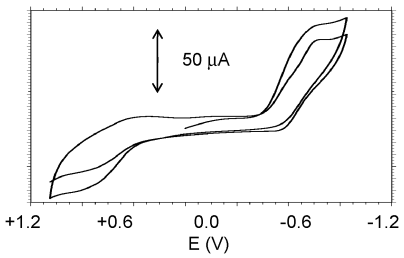


**Fig. 3** Cyclic voltammograms for **5**-modified glassy carbon electrodes immersed into $O_2$-saturated 0.10 M $Et_4NClO_4$/MeCN solution. Scan rate: 50 mV $s^{-1}$.

of a microparticulate deposit of the complex on a glassy carbon electrode. As can be seen in Fig. 3, in contact with $O_2$-saturated MeCN solutions, **5**-modified electrodes produce a sharp decrease of the anodic peak of the reversible $O_2/O_2^-$ couple, thus denoting that the superoxide ion electrochemically generated upon reduction of dissolved $O_2$[17] rapidly reacts with the manganese complex with concomitant abrupt decrease of the anodic signal. The $O_2/O_2^-$ couple is accompanied by an anodic wave at +0.70 V *vs.* AgCl/Ag, corresponding to the solid state oxidation of the parent $Mn^{II}$ complex (Fig. S3, ESI†). All these features denote the existence of a significant reactivity of the studied species with superoxide ion even under electrochemical activation conditions.

Table 1 also collects results of preliminary *in vitro* studies of the SOD activity using the nitro blue tetraazolium (NBT) reduction method[18] along with the reported data for the relevant MnSOD mimic M40403.

The values obtained are very promising ranking amongst the best values found in the literature.[19] As a matter of fact the $K_{cat}$ of $Mn^{II}$–**3** parallels the value reported for the pentaazamacrocycle M40403 that is one of the $Mn^{II}$ mimics that has up to now shown more potential.

The one order of magnitude difference in SOD activity between the manganese complexes of the two quinoline-containing ligands $Mn^{II}$–**2** and $Mn^{II}$–**3** deserves to be emphasized. The water molecule directly bound to manganese is a feature also observed in the native enzyme,[13] which seems to play a very significant role in the proton transfer steps of the mechanistic cycle and in the regulation of the electrode potential.

Preliminary studies with *Candida albicans* SC5314 in the presence of concentrations up to 0.5 mM of the here reported complexes do not reveal toxicity and show normal growth. Studies of the protective effects of these SOD mimics using *Saccharomyces cerevisiae* ATCC96687 and ATCC96688 deficient in Sod1p and Sod2p, respectively, are currently being carried out.[20]

We would like to thank MCINN (Spain) for financial support (Projects CONSOLIDER INGENIO CSD-2010-00065 and CTQ2009-14288-C04-01).

## Notes and references

1 (*a*) H. Fu, Y.-H. Zhou, W.-L. Chen, Z.-G. Deqing, M.-L. Tong, L.-N. Ji and Z.-W. Mao, *J. Am. Chem. Soc.*, 2006, **128**, 4924; (*b*) J. S. Valentine and P. J. Hart, *Proc. Natl. Acad. Sci. U. S. A.*, 2003, **100**, 3617.
2 K. J. Barnham and A. I. Bush, *Curr. Opin. Chem. Biol.*, 2008, **12**, 222.
3 (*a*) R. M. Lebovitz, H. Zhang, H. Vogel, J. Cartwright Jr., L. Dionne, N. Lu, S. Huang and M. Matzuk, *Proc. Natl. Acad. Sci. U. S. A.*, 1996, **93**, 9782; (*b*) S. Raha and B. H. Robinson, *Trends Biochem. Sci.*, 2000, **25**, 502.
4 D. P. Riley, *Chem. Rev.*, 1999, **99**, 2573.
5 (*a*) K. Aston, N. Rath, A. Naik, U. Slomczynska, O. F. Schall and D. P. Riley, *Inorg. Chem.*, 2001, **40**, 1779; (*b*) G.-F. Liu, M. Filipovic, F. W. Heinemann and I. Ivanović-Burmazović, *Inorg. Chem.*, 2007, **46**, 8825; (*c*) A. Dees, A. Zahl, R. Puchta, N. J. R. Van Eikema Hommes, F. W. Heinemann and I. Ivanović-Burmazović, *Inorg. Chem.*, 2007, **46**, 2459; (*d*) M. Tamura, Y. Urano, K. Kikuchi, T. Higuchi, M. Hirobe and T. Naguno, *J. Organomet. Chem.*, 2000, **611**, 586; (*e*) D. Zhang, D. H. Busch, P. L. Lennon, R. H. Weiss, W. L. Neumann and D. P. Riley, *Inorg. Chem.*, 1998, **37**, 956.
6 D. Salvemini, Z.-Q. Wang, J. L. Zweier, A. Samouilov, H. Macarthur, T. P. Misko, M. G. Currie, S. Cuzzocrea, J. A. Sikorski and D. P. Riley, *Science*, 1999, **286**, 304.
7 B. Verdejo, S. Blasco, E. García-España, F. Lloret, P. Gaviña, C. Soriano, S. Tatay, H. R. Jiménez, A. Doménech and J. Latorre, *Dalton Trans.*, 2007, 4726.
8 (*a*) T. J. Lotz and T. A. Kaden, *J. Chem. Soc., Chem. Commun.*, 1977, 15; (*b*) P. S. Pallavicini, A. Perotti, A. Poggi, B. Segui and L. Fabbrizzi, *J. Am. Chem. Soc.*, 1987, **109**, 5139; (*c*) V. Amendola, L. Fabbrizzi, M. Lichelli, C. Mangano, P. Pallavicini, L. Parodi and A. Poggi, *Coord. Chem. Rev.*, 1999, **192**, 649.
9 E. García-España, M. P. Clares, C. Soriano, S. Blasco, B. Verdejo and J. González, Patent Application Number P20093071L.
10 B. Verdejo, A. Ferrer, S. Blasco, C. E. Castillo, J. González, J. Latorre, M. A. Mañez, M. García Basallote, C. Soriano and E. García-España, *Inorg. Chem.*, 2007, **46**, 5707.
11 P. Gans, A. Sabatini and A. Vacca, *Talanta*, 1996, **43**, 1739.
12 W. B. Greenleaf, J. Jefferson, P. Perry, A. S. Hearn, D. E. Cabelli, J. R. Lepock, M. E. Stroupe, J. A. Tainer, H. S. Nick and D. N. Silverman, *Biochemistry*, 2004, **43**, 7038.
13 D. M. Stanbury, *Adv. Inorg. Chem.*, 1989, **33**, 70.
14 I. Batinic-Haberle, I. Spasojevic, R. D. Stevens, B. Bondurant, A. Okado-Matsumoto, I. Fridovich, Z. Vujaskovic and M. W. Dewhirst, *Dalton Trans.*, 2006, 617.
15 C. Muscoli, S. Cuzzocrea, D. P. Riley, J. L. Zweier, C. Thiemerman, Z.-Q. Wang and D. Salvemini, *Br. J. Pharmacol.*, 2003, **140**, 445.
16 F. Scholz, U. Schröder and R. Gulaboski, *Electrochemistry of Immobilized Particles and Droplets*, Springer, Berlin-Heidelberg, 2005.
17 (*a*) P. Cofre and D. T. Sawyer, *Anal. Chem.*, 1986, **58**, 1057; (*b*) P. S. Singh and D. H. Evans, *J. Phys. Chem. B*, 2006, **110**, 637.
18 (*a*) C. Beauchamp and I. Fridovich, *Anal. Biochem.*, 1971, **44**, 276; (*b*) L. W. Oberley and D. R. Spitz, in *Handbook of Methods of Oxygen Radical Research*, ed. R. A. Grenwald, CRC Press, Boca Ratón, USA, 1986, pp. 218; (*c*) J. Y. Zhou and B. Prognon, *J. Pharm. Biomed. Anal.*, 2006, **40**, 1143.
19 O. Iranzo, *Bioorg. Chem.*, 2011, **39**, 73–87.
20 M. González-Álvarez, G. Alzuet, J. Borrás, L. del Castillo Agudo, S. García-Granda and J. M. Montejo-Bernardo, *Inorg. Chem.*, 2005, **44**, 9424.

 